Available online at www.sciencedirect.com
ScienceDirect
ELSEVIER
International Journal of Machine Tools & Manufacture 47 (2007) 326–334
INTERNATIONAL JOURNAL OF MACHINE TOOLS & MANUFACTURE DESIGN, RESEARCH AND APPLICATION
www.elsevier.com/locate/ijmactool

Dynamics of the arch-type reconfigurable machine tool

Jaspreet Dhupia*, Bartosz Powalka, Reuven Katz, A. Galip Ulsoy

NSF Engineering Research Center for Reconfigurable Manufacturing Systems, University of Michigan, 2250 GGBL, 2350 Hayward Street, Ann Arbor, MI 48109-2125, USA

Received 14 July 2005; received in revised form 20 March 2006; accepted 23 March 2006
Available online 22 May 2006

Abstract

Reconfigurable manufacturing systems (RMS) address challenges in modern manufacturing systems arising from product variety and from rapid changes in product demand. This paper considers an arch-type reconfigurable machine tool (RMT) that has been built to demonstrate the basic concepts of RMT design. The arch-type RMT was designed to achieve customized flexibility and includes a passive degree-of-freedom, which allows it to be reconfigured to machine a family of parts. The kinematic and dynamic capabilities of the machine are presented, including the experimental frequency response functions (FRFs) and computed stability lobes of the machine in different configurations. A comparison of FRFs and stability lobes of the arch-type RMT reveals almost similar dynamic characteristics at different reconfiguration positions. These similar characteristics arise because the dominant mode where chatter occurs is due to the spindle–tool–tool holder assembly. Consequently, to ensure consistent dynamic behavior regardless of reconfiguration, a desirable dynamic design feature for RMTs is that the machine's structural frequencies are less dominant than the structural frequencies of the spindle, tool and tool holder.

Keywords: Dynamics; Stability lobes; Customization; Reconfiguration

1. Introduction

Traditional manufacturing systems can be classified as: (a) dedicated manufacturing systems (DMS)—designed to produce a specific part or (b) flexible manufacturing systems (FMS)—designed to accommodate a large variety of parts even though parts are not specified at the design stage. While DMS is economical when the output volumes are high for a manufactured product over a long period of time, FMS is more suited if the production volume is low and a large variety of parts are produced. Changing product demands in current markets makes DMS less desirable, but FMS lacks the efficiency and robustness of DMS, making it uneconomical for many production situations.

Reconfigurable manufacturing systems (RMSs), which aim to achieve '*exactly the capacity and functionality needed, exactly when needed*,' have garnered considerable attention in recent years [1–5]. Research has been done on design and operation of RMSs; lead-time; and ramp-up time reduction and open architecture controllers at various research centers in US, Europe and Japan [6–12]. Industry is also beginning to adopt and implement various aspects of RMS [13,14]. Indeed, it is becoming clear that reconfiguration will be an important aspect of many future manufacturing systems. Key characteristics of an RMS include: (1) modularity, (2) integrability, (3) convertibility, (4) customization, (5) scalability, and (6) diagnosibility. The more of these characteristics a manufacturing system possesses, the more reconfigurable it becomes.

An important issue is the appropriate 'granularity' of the modules in an RMS. For many manufacturing systems the basic module for reconfiguration will be a 3-axis CNC machine tool—a commodity product whose cost has significantly fallen in recent years, while accuracy and reliability have improved. However, in research one must consider a variety of alternatives. Consequently, this paper will discuss the concept of a reconfigurable machine tool (RMT), which brings the 'granularity' of reconfiguration down from the machine level to the component level. Reconfiguration at the component level, as in RMTs, raises

*Corresponding author. Tel.: +1 734 276 8010; fax: +1 734 615 0312.
E-mail address: jdhupia@umich.edu (J. Dhupia).

0890-6955/$ - see front matter
doi:10.1016/j.ijmachtools.2006.03.017

several difficult research issues such as costs, joints, accuracy and dynamic structural response. Nevertheless, the concept of an RMT brings many of the potential advantages of an RMS to the component level. Thus, it is useful to conduct research on RMTs, to assess weather some of the basic research challenges can be addressed, and if attractive application niches for RMTs can be developed. Consequently, our research group has designed and built several RMTs, including a table-top Cartesian 3-axis RMT, a reconfigurable inspection machine, and an arch-type RMT [3,15–20].

The purpose of this paper is to describe the so-called arch-type RMT, first demonstrated at the 2002 International Manufacturing Technology Show in Chicago, and to provide a brief description of the design concept, the design and construction, and dynamic characteristics of the machine. This paper describes the frequency response functions (FRFs) and experimentally verified analytical stability lobes for the machine at different reconfiguration positions. Cutting model estimation has also been carried out to evaluate the stability lobes of the machine. Contrary to predictions during the design stage of arch-type RMT [15,18], the dynamic performance of the machine does not vary significantly with reconfiguration position. The reason for this is discussed in the paper.

2. Background and methodology

2.1. Arch-type RMT: design and construction

The characteristics of customized flexibility on which the arch-type RMT design is based, makes the design procedure more involved than the design of a dedicated machine tool or a flexible CNC machine tool [17,20]. The functional design of the arch-type RMT is focused on the finish milling of cylinder head inclined surfaces. The tooling tolerances and process parameters were the same for all inclined surfaces. However, the surfaces to be milled are at different angles with respect to the horizontal: 30° (for V6 cylinder heads) and 45° (for V8 cylinder heads). A dedicated machine tool solution would need a customized station for each member of the part family. If a commercial CNC machine solution is sought, one would have to choose from available 5-axis CNC machines with orthogonal kinematics. In the arch-type RMT an alternative reconfigurable solution is presented where the machine is capable of 3-axis kinematics with one passive degree-of-freedom available for reconfiguration.

A detailed evaluation of various possible conceptual machine tool configurations was undertaken by Katz and Chung [15]. Based on workspace evaluation, finite element analysis (FEA) and research considerations the decision to go ahead with a side-mounted arch-type RMT (Fig. 1a) was taken. A detailed FEA analysis (Fig. 1b) was carried out on the final design and the calculated natural frequencies for lower structural modes of 45° reconfiguration position are shown in Table 1 [18]. Some of the alternative solutions to arch-type RMT considered were to achieve the passive degree for reconfiguration by pivoting the spindle housing or pivoting the worktable. The pivoted spindle housing designs (shown in Fig. 2) were not selected because of the limited workspace achieved by such machines at higher reconfiguration angles. The pivoted worktable was not chosen because of the concerns of compatibility of such a machine with most conveyor system environments in industry. The arch-type RMT (Fig. 3) was built by a commercial machine tool manufacturer, and was showcased in the International Manufacturing Technology Show, September 2002, Chicago [13].

2.2. Dynamics of machine tools

This paper describes the FRFs and the stability lobe diagrams for chatter for the arch-type RMT at the $\theta = 0°$ and 45° reconfiguration position, to investigate variations

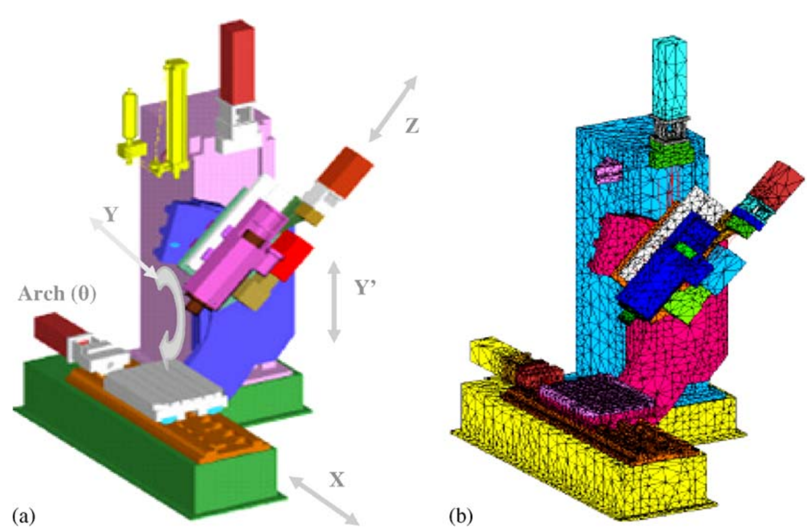

Fig. 1. Final design for RMT with its finite element model.

Table 1
Modal data for final RMT design

Mode #	Frequency (Hz)	Comments
1	36	Mainly due to weak connection between the ram and the arch.
2	53	Mainly due to column/base structure
3	60	Mainly due to a combination of weak connection between the ram and the arch, and stiffness of Y-axis
4	69	Mainly due to weak connection between the ram and the arch
5	72	Mainly due to a combination of weak connection between the ram and the arch, and stiffness of Z-axis

These data are valid only for a position of the machine in which: (a) spindle is half the way extended, i.e. 250 m, (b) ram is positioned at 45° angle, and (c) arch is positioned at the middle of its 775 mm stroke.

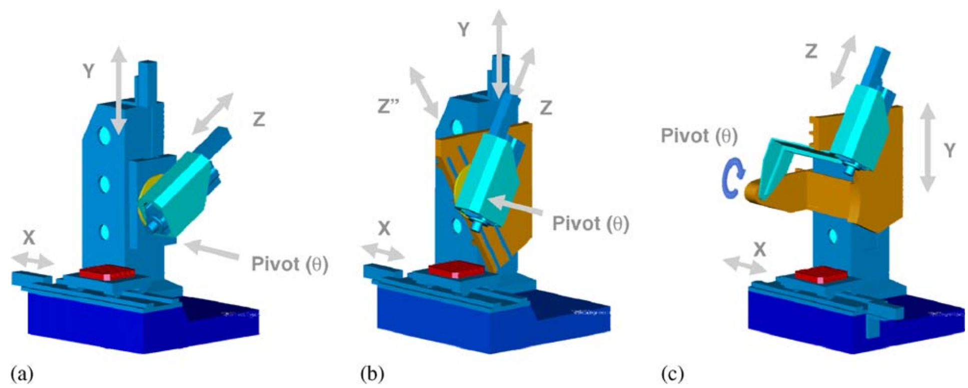

Fig. 2. Different pivot-type RMT design concepts.

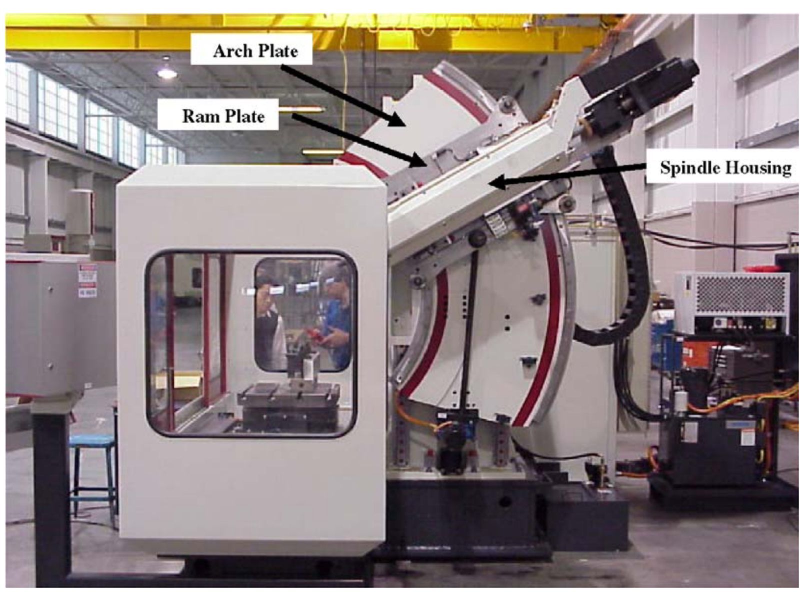

Fig. 3. Arch-type RMT.

in arch-type RMT dynamic performance. While the FRF gives the description of structural vibrations and stiffness of the machine tool [21], the stability lobes for chatter can be used as a direct assessment of the expected machining quality and productivity.

The FRF matrix, also known as the receptance matrix for the relative workpiece-machine tool vibration, $\mathbf{G}(i\omega)$, is the transfer function from the cutting force to the relative workpiece–machine displacement. $\mathbf{G}(\mathrm{i}\omega) = \mathbf{G_t}(\mathrm{i}\omega) - \mathbf{G_w}(\mathrm{i}\omega)$, where $\mathbf{G_t}(\mathrm{i}\omega)$ and $\mathbf{G_w}(\mathrm{i}\omega)$ are the FRF matrices of tool and workpiece, respectively. Let the displacement of the tool be $\mathbf{u_t}$ and that of the workpiece be $\mathbf{u_w}$. The cutting forces acting on the tool ($\mathbf{f_t}$) and the workpiece ($\mathbf{f_w}$) have the same magnitude but opposing directions (i.e. $\mathbf{f_t} = -\mathbf{f_w}$).

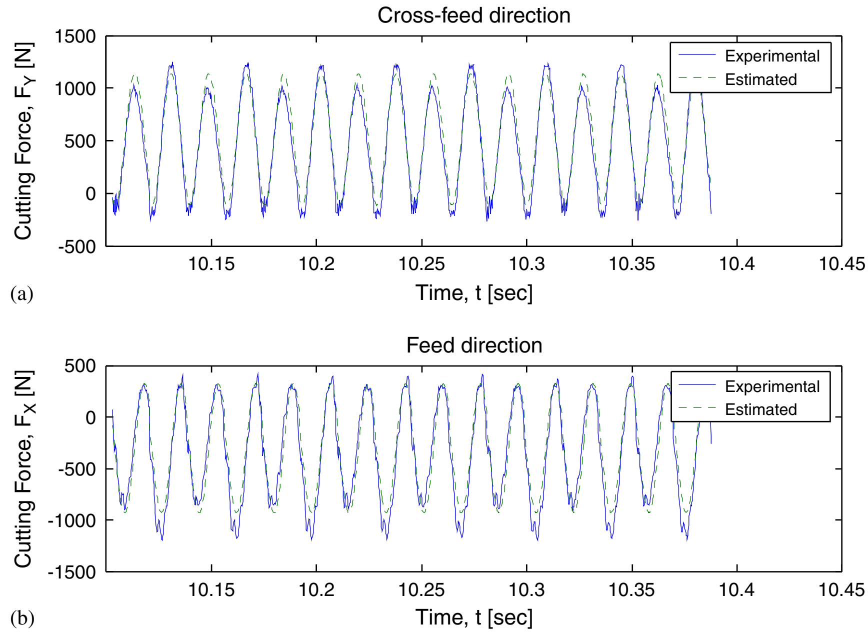

Fig. 4. Experimental and estimated cutting forces at $a_p = 3.3$ mm, $N = 1700$ RPM and $f_t = 7.2$ mm/s.

In this paper the workpiece is assumed rigid, and the assumption was verified by measuring the FRF of the workpiece and measuring the vibrations displacement of the workpiece during the cutting experiments. Thus, the relationship between the cutting force and vibrations at the tool tip become:

$$\mathbf{G}(\mathrm{i}\omega)\,\mathbf{f_t}(\mathrm{i}\omega) = \mathbf{u_t}(\mathrm{i}\omega). \tag{1}$$

In general, $\mathbf{G}(i\omega)$ would be a 3×3 matrix, as displacements and the force vector are defined in the three-dimensional Cartesian system. However in the milling process, the axial direction (Z) is typically much stiffer than the feed force direction (X) and the cross feed force direction (Y) (see Fig. 1). Therefore

$$\mathbf{G}(i\omega) = \begin{bmatrix} G_{XX}(\mathrm{i}\omega) & G_{XY}(\mathrm{i}\omega) \\ G_{YX}(\mathrm{i}\omega) & G_{YY}(\mathrm{i}\omega) \end{bmatrix}. \tag{2}$$

Here, G_{XX} and G_{YY} are FRFs that were experimentally determined by an impact hammer test. The off-diagonal cross coupling terms G_{XY}, G_{YX} in Eq. (2) are relatively small and are neglected.

The vibrations of the machine affect the quality of machining due to chatter (i.e., regenerative self excited vibrations). Chatter occurs due to the interaction of the workpiece and tool, which leads to vibrations near one of the structural modes. At some combinations of spindle speed and depth of cut, the cutting forces can become unstable and cause chatter. The analytical chatter prediction model presented by Altintas and Budak [22,23] gives the characteristic equation of the milling process and equates it to zero to find the stability limit. The characteristic equation for finding the stability limit for this system is

$$\det\left[\mathbf{I} - \frac{1}{2} K_{\mathrm{tc}}\, a_{\mathrm{p}}(1 - \mathrm{e}^{-\mathrm{i}\omega_{\mathrm{c}} T})\mathbf{A}_0\, \mathbf{G}(\mathrm{i}\omega_c)\right] = 0, \tag{3}$$

where a_{p} is the nominal depth of cut, K_{tc} is the tangential cutting coefficient, ω_{c} is the chatter frequency, T is the tooth passage period and $\mathbf{A}_0$ is the immersion dependent matrix which is a function of the cutting coefficients.

The cutting experiments were done for estimating the cutting coefficients and to verify the analytical stability lobes by verifying the regions of stability and instability. The cutting coefficients are constant for a given tool insert–workpiece combination and not affected by the change in machine structure. The axial cutting coefficients are not necessary for finding the stability lobes because the structure has been assumed rigid along the axial direction. Feed and cross-feed forces were measured while cutting in full immersion with two inserts only. The mechanistic cutting force model [22] for the milling cutting process is described as

$$\begin{aligned} F_X &= -K_{\mathrm{tc}}\, a_{\mathrm{p}} f_{\mathrm{t}} \sin\phi \sin\phi - K_{\mathrm{te}}\, a_{\mathrm{p}} \sin\phi \\ &\quad - K_{\mathrm{rc}}\, a_{\mathrm{p}} f_{\mathrm{t}} \sin\phi \cos\phi - K_{\mathrm{re}}\, a_{\mathrm{p}} \cos\phi, \\ F_Y &= K_{\mathrm{tc}}\, a_{\mathrm{p}} f_{\mathrm{t}} \sin\phi \cos\phi + K_{\mathrm{te}}\, a_{\mathrm{p}} \cos\phi \\ &\quad - K_{\mathrm{rc}}\, a_{\mathrm{p}} f_{\mathrm{t}} \sin\phi \sin\phi - K_{\mathrm{re}}\, a_{\mathrm{p}} \cos\phi. \end{aligned} \tag{4}$$

Knowing F_X, F_Y for different values of instantaneous cutter angular locations ϕ, the cutting coefficients K_{tc}, K_{te}, K_{rc} and K_{re} can be estimated using the least-squares approach. The forces F_X and F_Y are the components of $\mathbf{f_t}$ in Eq. (1), i.e., $\mathbf{f_t} = [F_X, F_Y]^{\mathrm{T}}$. The constants K_{tc} and K_{rc} arise due to the shearing action in the tangential and radial directions respectively. K_{te} and K_{re} are the corresponding

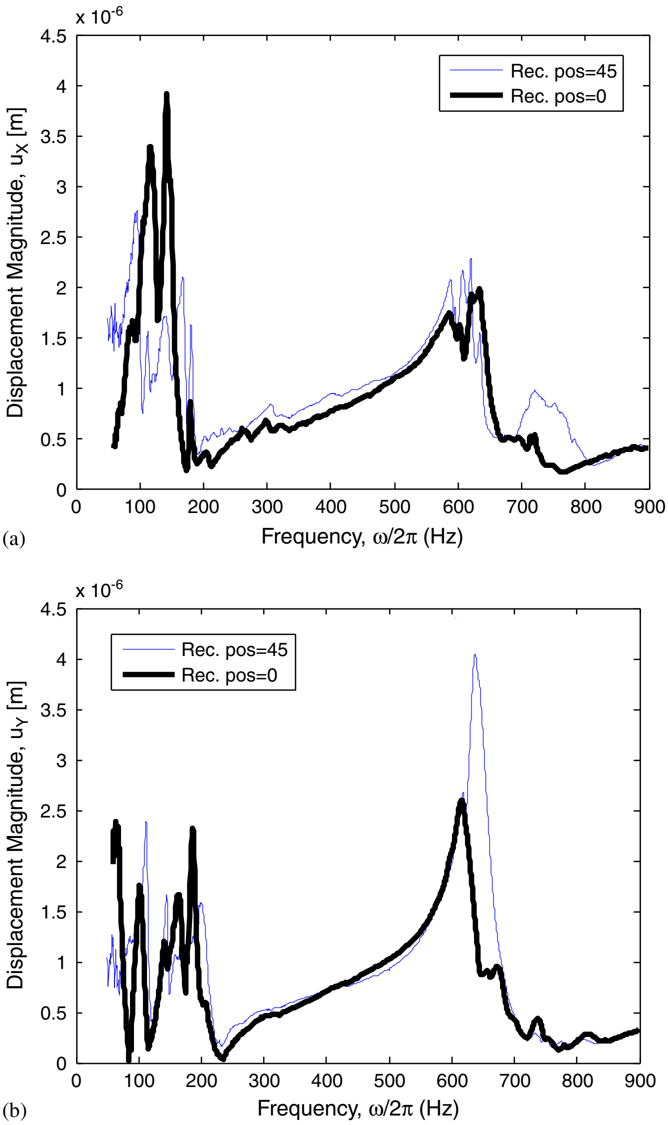

Fig. 5. Experimental arch-type RMT's tool FRF for 0° and 45° reconfiguration position with valenite V490 cutter. (a) Excitation in X, measured response in X direction. (b) Excitation in Y, measured response in Y direction.

edge constants, and f_t represents the feed per tooth. While the tangential cutting coefficient, K_{tc}, appears directly in Eq. (3), the matrix $\mathbf{A_0}$ is dependent on K_{rc}. The edge constants are needed for the cutting coefficient estimation.

All the cutting experiments were carried out using a Valenite V490 square shoulder end mill with rectangular inserts (outer diameter: 50.8 mm, insert width: 15.875 mm) and AISI 1018 steel. While two inserts were used for cutting model estimation, stability lobe diagram and chatter estimation was carried out for four inserts. Since the goal of the paper is to provide a comparison between the different reconfiguration positions of the arch-type RMT, the tool and the workpiece were kept the same in different reconfiguration positions.

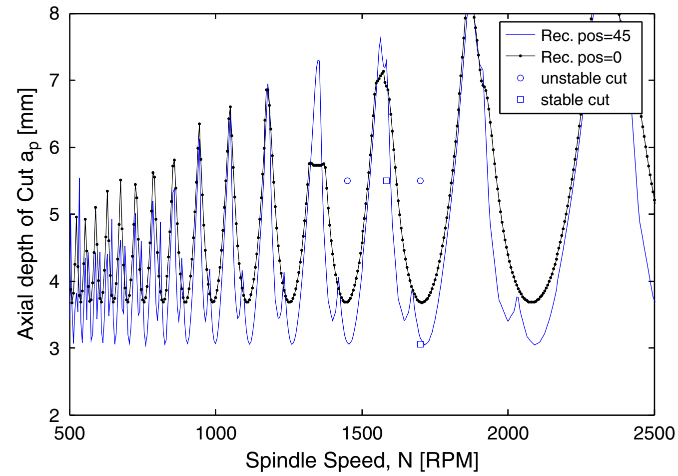

Fig. 6. Analytical stability lobes showing the regions of stability and instability verified by cutting experiments.

3. Results and discussion

3.1. Cutting model

Fig. 4 shows the results for force measurements while cutting AISI 1018 steel at depth of cut, $a_p = 3.3$ mm, spindle speed, $N = 1700$ RPM and feed per tooth, $f_t = 0.127$ mm/tooth. The cutting coefficients determined by the least-squares method, using the force signal after the initial transients due to the tool entering the workpiece decayed were

$$K_{tc} = 2309.94\,\text{N/mm}^2, \quad K_{rc} = 1337.79\,\text{N/mm}^2,$$
$$K_{te} = 24.79\,\text{N/mm}, \quad K_{re} = 17.69\,\text{N/mm}.$$

The correlation factors for the estimated and experimental data have large values of 0.98 for feed (X) direction and 0.96 for cross feed (Y) direction, indicating a good fit.

3.2. Frequency response functions

Modal tests were performed on the arch-type RMT at various reconfiguration positions. Fig. 5 shows the FRFs G_{XX} and G_{YY} for the $\theta = 0^\circ$ and $\theta = 45^\circ$ reconfiguration positions. It may be noted that the FRFs have very similar pattern at the higher frequencies (>250 Hz), but at lower frequencies the patterns are quite different. This is because the lower frequencies arise from the structure of the machine tool, i.e., lower frequency are primarily due to structural modes other than the spindle, tool and tool holder. Since the structure of an RMT changes from one reconfiguration position to another, the lower frequencies (<250 Hz) are affected significantly. The magnitude of the FRF at $\theta = 0^\circ$ is higher than that of $\theta = 45^\circ$ at lower frequencies. The arch plate (Fig. 3) has to move up at $\theta = 0^\circ$ to cut the workpiece which is kept at the same level. Since the arch plate makes up a large fraction of the mass

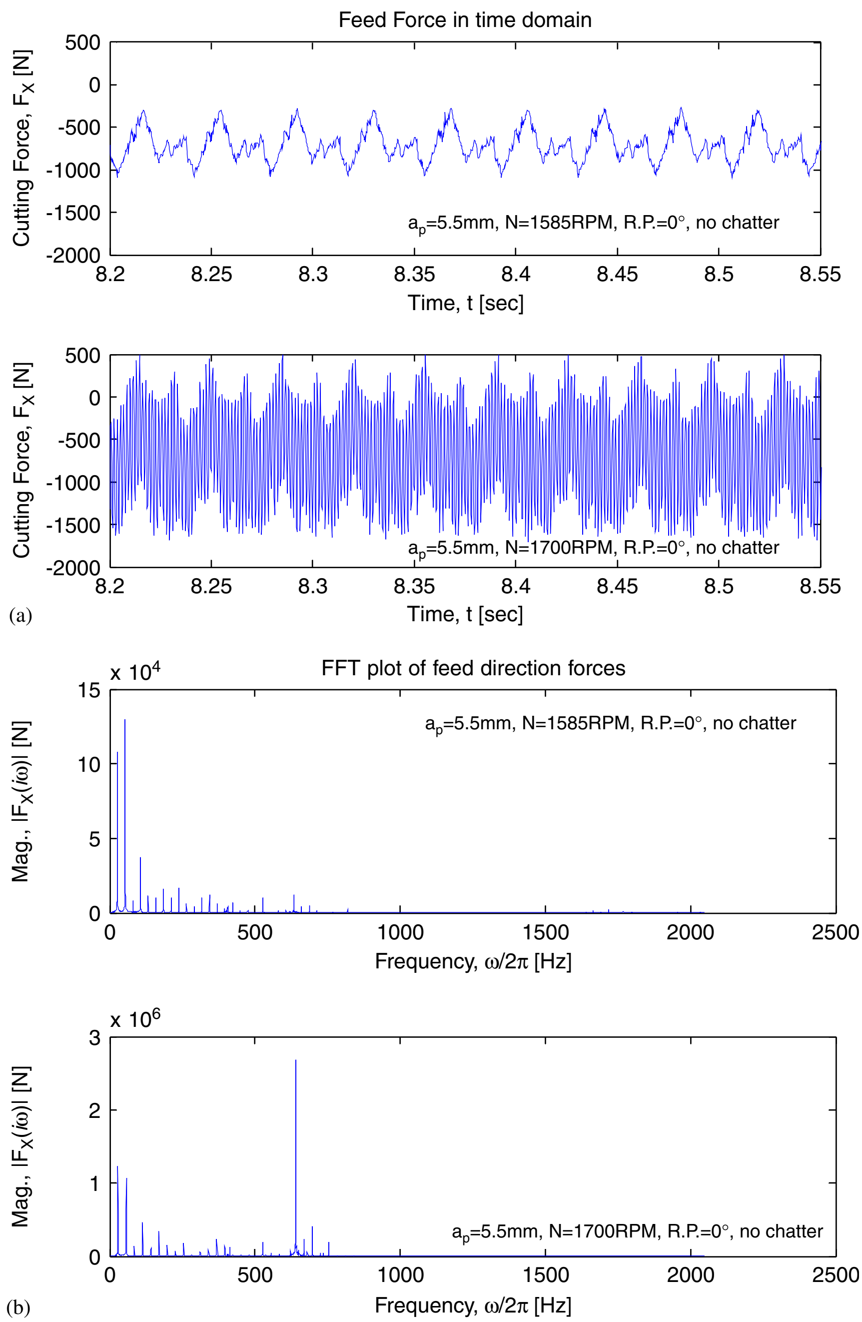

Fig. 7. (a) Experimental F_x plots for stable and unstable conditions at reconfiguration position, $\theta = 0°$ and (b) corresponding FFTs of the force data.

of the machine, the displacement of the arch on the machine has the most significant effect on the FRF of the machine structure. The higher the arch plate moves, less stiff the structure becomes. Thus, in this case, the configuration at $\theta = 0°$is less stiff at lower frequencies modes, than the configuration at $\theta = 45°$ since the arch plate is located higher for $\theta = 0°$. A large hammer (bandwidth 0–600 Hz) was used to study the lower frequencies range of the structural FRF of the machine. The lowest dominant natural frequency of the machine found was around 60 Hz.

3.3. Stability lobes

The analytical stability lobes generated for $\theta = 0°$ and $45°$ are shown in Fig. 6. Various cutting experiments were done to verify the regions of stability and instability based on these lobes. These points are marked on the stability lobe diagram and validate the stability lobe prediction. The cutting experiments results for $\theta = 0°$ and $45°$ were similar at various cutting conditions. The analytical stability lobes indicate that the chatter occurs for the $\theta = 45°$ configuration at a smaller depth of cut compared to that for the

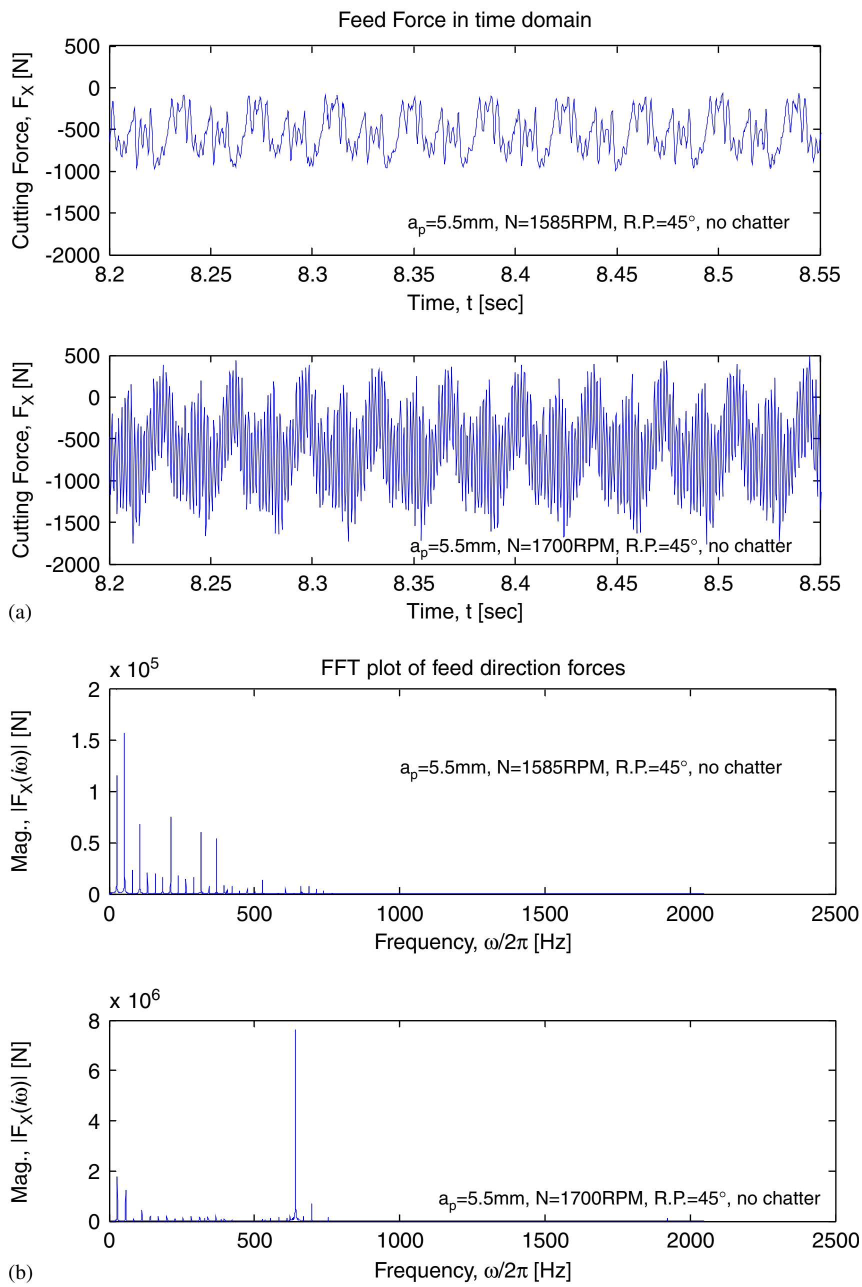

Fig. 8. (a) Experimental F_x plots for stable and unstable conditions at reconfiguration position, $\theta = 45^\circ$ and (b) corresponding FFTs of the force data.

$\theta = 0^\circ$. This is because the FRF plot has a higher magnitude (4×10^6 N/m) near the 640 Hz frequency for the $\theta = 45^\circ$ reconfiguration position.

The occurrence of chatter was verified from the measured force in the time domain as well as from frequency domain plots. Figs. 7a and b shows the cutting force plots and FFT of the cutting force signal for the $\theta = 0^\circ$ reconfiguration position. It can be seen from the force plots, that the cutting force profile is not clearly visible when the cutting was carried out at $a_p = 5.5$ mm, $N = 1700$ RPM. This indicates the presence of chatter at these cutting conditions. The cutting process at $a_p = 5.5$ mm, $N = 1585$ RPM is stable. The chatter was also be verified from the fast Fourier transform (FFT) of the force data. The magnitude of force at the tooth pass frequency is smaller than the magnitude of force at a frequency near one of the natural frequency of the machine structure (i.e., the chatter frequency), which verifies the existence of chatter.

The cutting experiments did not show very different results for the two reconfiguration positions (Figs. 7 and 8). This is because the chatter occurs near the natural frequency 640 Hz, which is expected to come from the spindle–tool–tool holder assembly. Since this sub-module is not affected during the reconfiguration process, the dynamic contribution due to it would be similar in different reconfiguration positions. The small difference, which results in the $\theta = 0^\circ$ reconfigurable position having larger

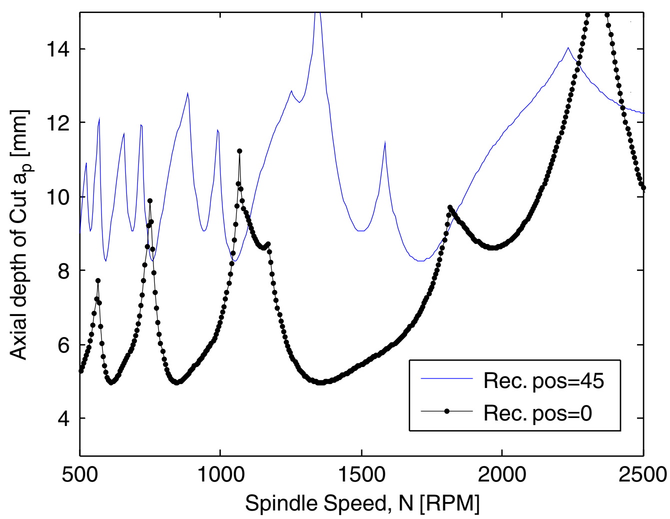

Fig. 9. Analytical lobes generated by structural modes only.

pockets of instability, was found to be because of higher damping associated with this mode at the $\theta = 0^\circ$ reconfiguration position. The higher damping in this reconfiguration position is the result of the change in distribution of weight at various joints which connect the spindle housing and spindle with the ram plate (Fig. 3). If the mode at this 640 Hz frequency is neglected while computing the stability lobes we get very different results for the analytical stability lobes for $\theta = 0^\circ$ and 45° reconfiguration positions (Fig. 9). These results would be relevant if the spindle–tool–tool holder is stiffer. A similar variation in stability lobe diagram would also be observed if the structure of the machine tool is made more compliant. Since an RMT is designed around a part family, a consistent dynamic performance of the machine across a part family is also desired. The reconfiguration of an RMT will affect the dynamic performance significantly if the structural frequencies are dominant enough to cause chatter near one of the structural frequencies. These results could have been verified by cutting experiments at lower spindle speeds ($<$1000 RPM). However, the machine does not have enough power for such cutting tests. The arch-type RMT is designed for end milling which is often carried out at high spindle speeds and, therefore, does not has enough power at low spindle speeds.

4. Concluding remarks

The arch-type RMT was designed to achieve customized flexibility for a family of parts: cylinder heads for V6 and V8 automotive engines. It is a 3-axis CNC machine tool that has an additional passive rotational degree-of-freedom. This paper describes the dynamic characteristics of the arch-type RMT as it is changed from one reconfiguration position ($\theta = 0^\circ$) to another ($\theta = 45^\circ$). In this case the performance of the arch-type RMT does not change much when the machine tool is reconfigured from one position to another. This is because chatter occurs at 640 Hz, a frequency that arises due to the spindle–tool–tool holder assembly. A useful insight gained for designing RMT is to have a structure that is stiff enough at all reconfigurable positions such that the dominant frequency of the structure in the FRF is due to the spindle–tool–tool holder assembly. This ensures a uniform performance of the machine tool across the part family.

Various RMT design alternatives that were considered before selecting the arch-type RMT configuration were discussed in Section 2.1 (see Fig. 2). Those alternates were not selected because of the ease of use of the arch-type configuration and considerations apart from dynamics. While in this particular case, we do not observe significant changes in dynamic performance as machine is changed from one reconfiguration position to another, if the spindle–tool–tool holder assembly was made stiffer, the arch-type RMT performance can vary significantly as the arch plate is moved relative to the *Y*-column. Therefore, it is important to recognize the trade-offs between dynamic capabilities and other design considerations in the design of RMTs.

Acknowledgments

The authors are pleased to acknowledge the financial support of the NSF Engineering Research Center for Reconfigurable Manufacturing Systems (NSF Grant # EEC-9529125), and the assistance of Mr. Steve Erskine with the machining experiments.

References

[1] S. Ashley, Manufacturing firms face the future, Manufacturing Engineering (1997) 70–74.

[2] Y. Koren, U. Heisel, F. Jovane, T. Moriwaki, G. Pritschow, G. Ulsoy, H. Van Brussel, Reconfigurable manufacturing systems, CIRP Annals—Manufacturing Technology 48 (2) (1999) 527–540.

[3] Y. Koren, S. Kota, Reconfigurable machine tool, U.S. Pat. # 5,943,750, The Regents of the University of Michigan, USA, 1999.

[4] Y. Koren, A.G. Ulsoy, Reconfigurable manufacturing system having a production capacity method for designing same and method for changing its production capacity, U.S. Pat. # 6,349,237, The Regents of the University of Michigan, USA, 2002.

[5] M.G. Mehrabi, A.G. Ulsoy, Y. Koren, Reconfigurable manufacturing systems: key to future manufacturing, Journal of Intelligent Manufacturing 11 (4) (2000) 403–419.

[6] F.M. Asl, A.G. Ulsoy, Stochastic optimal capacity management in reconfigurable manufacturing systems, CIRP Annals—Manufacturing Technology 52 (1) (2003) 371–374.

[7] T. Fakuda, T. Ueyama, Autonomous behavior and control, in: Proceedings of IEEE International Conference on Robotics and Automation, 1993.

[8] F. Jovane, Y. Koren, C.R. Boer, Present and future of flexible automation: towards new paradigms, CIRP Annals—Manufacturing Technology 52 (2) (2003) 543–560.

[9] C.J.J. Paredis, H.B. Brown, P.K. Khosla, Rapidly deployable manipulator system, in: Proceedings of the 1996 13th IEEE International Conference on Robotics and Automation, part 2 (of 4), Minneapolis, MN, 1996, pp. 1434–1439.

[10] G. Pritschow, Y. Altintas, F. Jovane, Y. Koren, M. Mitsuishi, S. Takata, H. Van Brussel, M. Weck, K. Yamazaki, Open controller

architecture—past, present and future, CIRP Annals—Manufacturing Technology 50 (2) (2001) 463–470.

[11] A.S. Yigit, A.G. Ulsoy, Dynamic stiffness evaluation for reconfigurable machine tools including weakly non-linear joint characteristics, Proceedings of the Institution of Mechanical Engineers, Part B: Journal of Engineering Manufacture 216 (1) (2002) 87–101.

[12] A.S. Yigit, A.G. Ulsoy, A. Allahverdi, Optimizing modular product design for reconfigurable manufacturing, Journal of Intelligent Manufacturing 13 (4) (2002) 309–316.

[13] Anonymous, An easier way to machine? Manufacturing Engineering 129 (Sept 2002) 39.

[14] J. DeGaspari, All in the family, Mechanical Engineering 124 (2002) 56–58.

[15] R. Katz, H. Chung, Design of an experimental reconfigurable machine tool, Japan–USA Symposium on Flexible Automation, Ann Arbor, MI, 2000.

[16] R. Katz, Y.-M. Moon, Virtual arch type reconfigurable machine tool design: principles and methodology, ERC RMS, The University of Michigan, Ann Arbor, 2000, p. 34.

[17] R.G. Landers, B.-K. Min, Y. Koren, Reconfigurable machine tools, CIRP Annals—Manufacturing Technology 50 (1) (2001) 269–274.

[18] J. Manjunathaiah, A. Saeedy, Design and engineering of the reconfigurable machine tool, Final Report, Lamb Technicon, Lx-0445, 1999.

[19] Y.-M. Moon, Reconfigurable machine tool design: theory and application, Mechanical Engineering, University of Michigan, Ann Arbor, 2000, p. 166.

[20] Z.J. Pasek, S. Badrawy, Z. Li, K.-G. Ahn, Challenges and opportunities in the design of reconfigurable machine tools, Japan–USA Symposium on Flexible Automation, Hiroshima, Japan, 2002.

[21] D.J. Ewins, Modal testing: theory and practice, Letchworth, New York, Research Studies Press, Hertfordshire, England, 1984.

[22] Y. Altintas, Manufacturing automation: metal cutting mechanics, machine tool vibrations, and CNC design, Cambridge University Press, Cambridge, 2000.

[23] E. Budak, Y. Altintas, Analytical prediction of chatter stability in milling—part I: general formulation, part II: application of the general formulation to common milling systems, Proceedings of the 1995 ASME International Mechanical Engineering Congress and Exposition, part 1 (of 2), 12–17 November 1995, San Francisco, CA, USA, 1995, pp. 545–565.